C-kit+VEGFR-2+ Mesenchymal Stem Cells Differentiate into Cardiovascular Cells and Repair Infarcted Myocardium after Transplantation

Pei Zhou
Shanghai Medical University: Fudan University
Hai-feng Zhang
Shanghai Medical University: Fudan University
Yong-li Wang
Shanghai Medical University: Fudan University
Ping Tao
Shanghai Medical University: Fudan University
Yu-zhen Tan (yztan@shmu.edu.cn)
Shanghai Medical University: Fudan University https://orcid.org/0000-0001-7848-2132
Hai-jie Wang
Shanghai Medical University: Fudan University

Research Article

Keywords: c-kit, VEGFR-2, Mesenchymal stem cells, Stem cell transplantation, Myocardial infarction

Posted Date: January 11th, 2022

DOI: https://doi.org/10.21203/rs.3.rs-1235054/v1

Abstract

Background: Resent preclinical studies and clinical trails prove that transplantation of mesenchymal stem cells (MSCs) is a promised therapy for ischemic diseases. However, the properties of c-kit$^+$ cells in MSCs remain unclear. We investigated the differential potential of c-kit$^+$VEGFR-2$^+$ MSCs and evaluated their effects on repairing the infarcted myocardium after transplantation.

Methods: c-kit$^+$VEGFR-2$^+$ MSCs were isolated from rat bone marrow. Gene expression profile of the cells was examined with RNA-sequencing. Differential potential of the cells was determined after induction with VEGF, TGF-β and BMP-2 for 2 weeks. Improvement of cardiac function and repair of the infarcted myocardium were assessed at 4 weeks after transplantation of the cells preconditioned with hypoxia and serum deprivation.

Results: Gene expression profile revealed that the upregulated genes are enrichment of genes related to immune process and cell differentiation. The cells represented a potential of differentiation towards endothelial cell, smooth muscle cells and cardiamyocytes. In hypoxic condition, secretion of VEGF, SCF and SDF-1α from the cells was increased. VEGF and SCF promoted proliferation and migration of the cells. VEGF could induce the cells to incorporate to the microvessels. After transplantation of the preconditioned cells into the infarcted myocardium, cardiac function was improved, scar size of the infarcted myocardium was decreased, and angiogensis and myocardium repair were enhanced significantly. With preconditioning and delivery by fibrin gel, survival of the cells in the ischemic tissue was augmented.

Conclusion: These results suggest that c-kit$^+$VEGFR-2$^+$ MSCs have a potential of differentiation towards cardiovascular cells. SCF/c-kit and VEGF/VEGFR-2 singnalling pathways regulate proliferation, migration and differentiation of the cells. Transplantation of c-kit$^+$VEGFR-2$^+$ MSCs may enhance repair of the infarcted myocardium effectively.

Background

Myocardial infarction (MI) is a leading cause of death of the cardiovascular diseases worldwide. The overall prevalence for MI is 2.8% in US adults. MI prevalence is 4.0% for men and 1.8% for women [1].According to investigation of the European Society of Cardiology, one in six men and one in seven women in Europe will die from MI. However, despite improvements in pharmacological and interventional treatments, one in three men and one in four women die within a year of their first MI [2].

After the occlusion of a coronary artery, the resulting ischaemia can be severe leading to the death of both cardiomyocytes and non-myocytes locally, followed by local inflammation, degradation of extracellular matrix, scar formation and remodelling of the ventricular wall. The heart with MI may lose one billion cardiomyocytes, approximately 25% of its mass [3]. The current approach to the treatment of myocardial infarction involves early revascularisation with percutaneous coronary intervention or

coronary artery bypass grafting, followed by the medical management of atherosclerotic risk factors, late ventricular remodelling and cardiac arrhythmias. While the mammalian heart appears capable of endogenous regeneration at the early neonatal stage, this capacity is lost shortly after birth [4]. In human heart, renewal of cardiomyocytes is up to 1% per year at the age of 25 to 0.45% at the age of 75 [5]. Over the past decade, stem cell transplantation has emerged as a promising therapy for myocardial regeneration [6]. In several candidate stem cells, cardiac stem cells (CSCs) and mesenchymal stem cells (MSCs) have been considered as safe and reliable cell populations for cardiac transplantation [7].

c-kit$^+$ CSCs are characterized by a potential to differentiate toward cardiovascular cells though cardiomyogenic potential is controversial [8]. c-kit (as known as CD117) is a tyrosine kinase receptor that activates a downstream signaling cascade on binding to stem cell factor (SCF). c-kit regulated cardiomyocyte terminal differentiation and promoted CSC differentiation [9]. c-kit$^+$Nkx2.5$^+$ cells isolated from mouse embryonic heart possessed the capacity for differentiation into cardiomyocytes and smooth muscle cells [10]. Lin$^-$c-kit$^+$ cells isolated from rat heart [11] and human myocardial sample of cardiac surgery [12] are self-renewing, clonogenic and multipotent, giving rise to cardiomyocytes, endothelial cells, and smooth muscle cells. The number of c-kit$^+$Nkx2.5$^+$GATA4$^+$ cells increased significantly after cardiac injury [13]. Neonatal c-kit$^+$ cells had a cardiomyogenic potential, while this ability was lost in adult c-kit$^+$ cells [14]. Endogenous c-kit cells minimally contribute to cardiomyogenesis during neonatal and adult heart regeneration [15, 16]. Interestingly, transplantation of Lin$^-$c-kit$^+$ CSCs [11] or CD45$^-$c-kit$^+$ CSCs [17] was resulted in robust cardiomyogenesis and angiogenesis in the infarcted myocardium. It is worth noting that c-kit, in itself, does not define a specific marker for CSCs, and also expressed on other cells such as mast cells [18] and hematopoietic cells [19]. Lin$^-$CD45$^-$c-kit$^+$ cells only represented ≤10% of the adult rat c-kit$^+$ cardiac cells [17]. If resident CSCs are identified with c-kit expression alone, their potential to differentiate towards cardiovascular cells and effects in cardiomyocytic regeneration is probably misestimated.

MSCs are relatively easy to isolate from bone marrow or adipose tissue and can be expanded significantly ex vivo, exhibiting the properties of low immunogenicity and immunosuppression [20]. Regardless of the debated potential to generate cardiomyocytes in vivo, MSCs can differentiate towards cardiomyocytes, vascular smooth muscle and endothelial cells. Preclinical and clinical trails prove that MSCs can improve cardiac function and structure [21, 22]. Recent studies have suggested that there is a population of c-kit$^+$ cells having a cardiac regenerative potential in bone marrow cells. Intramyocardial injection of Lin$^-$c-kit$^+$ bone marrow cells promoted myocardial regeneration, ameliorating the outcome of MI [23]. After intracoronary injection of autologous c-kit$^+$ mononuclear cells isolated from bone marrow, cardiac function was improved, and pathological remodeling was attenuated [24]. c-kit$^+$ cells isolated from bone marrow-derived MSCs had a potential to differentiate towards cardiomyocytes. Preinduction with bone morphogenetic protein-2 (BMP-2) enhanced cardiomyogenic differentiation of c-kit$^+$ MSCs and repair of infarcted myocardium [25]. However, properties of c-kit$^+$ MSCs and their effect on myocardium repair need further investigation.

This investigation was designed to sort c-kit-positive and VEGFR-2 (vascular endothelial growth factor receptor-2)-positive cells from rat bone marrow-derived MSCs, and assess biological characteristics of c-kit$^+$VEGFR-2$^+$ MSCs and evaluate their effects on repairing the infarcted myocardium after transplantation. Here, we demonstrate that c-kit$^+$VEGFR-2$^+$ MSCs have a potential of differentiation towards cardiovascular cells. c-kit$^+$VEGFR-2$^+$ MSCs can effectively repair the infarcted myocardium through their differentiation and paracrine after transplantation.

Methods

Isolation of c-kit$^+$VEGFR-2$^+$ MSCs

Isolation of MSCs from bone marrow of Sprague-Dawley (SD) rats (2–4 weeks) was performed as described previously [26] with minor modification. The protocol was permitted by the law of the People's Republic of China on the Protection of Wildlife and approved by the Institutional Animal Care Committee of Fudan University. Briefly, bone marrow cells in the femurs and tibias were flushed out with PBS supplemented with 5 mM ethylene diamine tetraacetic acid (EDTA). The mononuclear cells in the bone marrow cells were isolated by Percoll (GE Healthcare, Leics, UK) gradient centrifugation, and then incubated with Dulbecco's modified Eagle's medium (DMEM; Hyclone, Logan, UT, USA) supplemented with 15% fetal bovine serum (FBS; Carlsbad, CA, USA) for 24 hrs. The non-adherent cells were discarded, the adherent cells were used as MSCs. The cells at the second passage were digested using 0.25% trypsin–EDTA (Thermo Fisher Scientific, Waltham, MA, USA) for 10 min at 4^{o}C and then resuspended in 1% bovine serum albumin (BSA, Amresco, Solon, OH, USA). After centrifugation, the cells were incubated with mouse anti-rat c-kit antibody (1:100) and polyclonal rabbit anti-rat VEGFR-2 antibody (1:200, Santa Cruz Biotechnology, Dallas, TX, USA) for 50 min at 4 ^{o}C. The cells were washed with 0.5% BSA and then incubated with Alexa Fluor 488 goat anti-rabbit IgG (1:100) and Alexa Fluor 647 goat anti-mouse IgG (1:400; Jackson ImmunoResearch Laboratories, West Grove, PA, USA) for 30 min at 4^{o}C. After washing twice with PBS, the cells were suspended with DMEM containing 2.5% FBS, and c-kit$^+$VEGFR-2$^+$ MSCs were sorted by a fluorescence-activated cell sorter (Beckman Coulter, Fullerton, CA, USA). The sorted cells were incubated with the complete medium, and the medium was changed every 3 days. c-kit$^+$VEGFR-2$^+$ MSCs at passage 3–6 were used in the following experiments.

RNA-sequencing

For examining biologic characteristics of c-kit$^+$VEGFR-2$^+$ MSCs, total RNA of c-kit$^+$VEGFR-2$^+$ and c-kit$^+$VEGFR-2$^-$ MSCs was extracted using the TRIzol Reagent Kit (Invitrogen) respectively. The samples were processed following the manufacturer's instructions (BGI Tech Solutions, Shenzhen, China). In brief, the target RNA was obtained after purification by mRNA enrichment using Oligo (dT) magnetic beads. Fragment target RNA was reverse transcribed into double-strand cDNA. After end repair and bubble adapter ligation, cDNA was amplified. PCR product was denatured by heat and cyclized to establish DNA library. Primary sequencing data (raw data) was acquired by Illumina HiSeq 2000 (Illumina, Santiago, CA,

USA). After filtering raw data to clean data, reads were aligned to genome reference. Bowtie2 was used to map clean reads to Rattus norvegicus. Differentially expressed genes were screened using Possion distribution with the fragments assigned per kilobase of target per million mapped reads (FPKM) method. Gene ontology (GO) was used to recognize the main biological functions of the two subpopulations of c-kit$^+$ cells. Moreover, GO functional annotation and enrichment analysis was used to compare the molecular functions and biological processing of the cells in two subpopulations. The pathways enriched with differentially expressed genes were made with Database of Kyoto Encyclopedia of Genes and Genomes (KEGG) [27].

Examination of proliferation and migration of the cells

c-kit$^+$VEGFR-2$^+$ MSCs were divided into vehicle, VEGF (vascular endothelial growth factor), SCF and VEGF + SCF groups. In VEGF and SCF groups, 10 ng/ml VEGF (Peprotech, Rocky Hill, NJ, USA) and 50 ng/ml SCF (Peprotech) were added in the medium respectively. After treatment with the growth factors for 24 hrs, the cells were incubated with rabbit anti-rat ki67 antibody (1:200; Abcam, Cambridge, UK), followed by Alexa Fluor 594-labelled goat anti-rabbit IgG (Jackson ImmunoResearch Laboratories). Ki67-positive cells were counted with a fluorescent microscope. Migration of the cells was assessed by transwell assay. The experimental grouping is the same as above. The diameter of the pores of the polyethylene terephthalate membrane in the transwell (Becton Dickinson, Franklin Lakes, NJ, USA) is 8 μm. The cells were seeded on the upper chamber, and the medium supplemented with the growth factors was added into the lower chamber. After incubation for 12 h, the cell insert was taken out and stained with 10% Giemsa. The cells on the upper chamber were wiped with tissue paper, and then the cells migrated into the lower chamber were counted. Three repeated experiments were performed.

Tube formation assay

The incorporation capacity of the c-kit$^+$VEGFR-2$^+$ cells into tube-like structures formed by pulmonary microvascular endothelial cells was accessed using previous method [28]. The lungs of SD rats (two-weeks old) were removed and put into pre-iced HBSS. After removing the pleura, the tissue near the border of the lung was cut into 1 mm^3 pieces. The tissue masses were incubated with DMEM in gelatin-coated wells for one week. The migrated endothelial cells were harvested, and then incubated in 24-well plate coated with Matrigel (3:2 in DMEM; BD Biosciences, San Jose, CA, USA). After capillary-like structures were formed, c-kit$^+$VEGFR-2$^+$ cells labelled with Dil (Beyotime Biotech, Haimen, Jiangsu, China) were added, and continued to be incubated for 4 hrs. c-kit$^+$VEGFR-2$^+$ cells incorporated into the capillary-like structures were counted with a fluorescent microscope. Five fields were selected randomly in each group. The experiment was repeated for four times. In VEGF group, c-kit$^+$VEGFR-2$^+$ cells were pretreated with 10 ng/ml VEGF for 2 hrs.

Reverse transcription-polymerase chain reaction (RT-PCR)

For accessing differentiation of c-kit$^+$VEGFR-2$^+$ MSCs towards endothelial cells, smooth muscle cells and cardiomyocytes, the cells were divided into VEGF, TGF-β (transforming growth factor-β) and BMP-2

groups. Total RNA was collected with the TRIzol Reagent Kit. After mRNA were reverted to cDNA using Primescript RT Reagent Kit with gDNA Eraser (Takara Biotechnology, Otsu, Japan), cDNA was amplified with PCR assay. In VEGF group, the cells were treated with 10 ng/ml VEGF for 2 weeks. Expression of *CD31* and *vWF* (von Willebrand factor) in the cells was analyzed by 1.2% agarose gel electrophoresis and visualized under ultraviolet light. In TGF-β group, the cells were treated with 2 ng/ml TGF-β (Peprotech) for 2 weeks. Expression of *α-SMA* (*α-smooth muscle actin*) and *CNN1* (*calponin 1*) in the cells was analyzed. mRNAs of the femoral artery from SD rat were used as positive controls in VEGF and TGF-β groups. In BMP-2 group, the cells were treated with 10 ng/ml BMP-2 (Peprotech) for 2 weeks. Expression of *Nkx2.5* and *GATA-4* in the cells was detected. mRNAs of the myocardium from SD rat were used as positive controls. The experiment was repeated for three times. The sequences of the primers were shown in Table S1.

Differentiation of c-kit$^+$VEGFR-2$^+$ MSCs was also examined with immunostaining. The cells induced with VEGF were incubated with mouse anti-rat CD31 antibody (1:200; Abcam) overnight, and then incubated with Alexa Fluor 594 goat anti-mouse IgG (1:400; Jackson ImmunoResearch Laboratories). The cells induced with TGF-β were incubated with mouse anti-rat α-SMA (1:200) and rabbit anti-rat desmin (1:100; Abcam) overnight, followed with Alexa Fluor 594 goat anti-mouse IgG (1:400) and Alexa Fluor 488 goat anti-rabbit IgG (1:200; Jackson ImmunoResearch Laboratories) respectively. After induction with BMP-2, the cells were incubated with mouse anti-rat cTnT (cardiac troponin T; 1:200) and rabbit anti-rat Cx43 (connexin-43; 1:200; Santa Cruz Biotechnology). The differentiated cells were viewed with a fluorescence microscope.

Enzyme-linked immunosorbent assay (ELISA)

Cytokine secretion of c-kit$^+$VEGFR-2$^+$ MSCs after treatment with hypoxia was detected with ELISA. The cells were incubated in a hypoxia chamber with 1% O_2, 5% CO_2 and 94% N_2 for 12 hrs. After the supernatants were collected, the cytokines were detected using VEGF, SCF and SDF-1α (stromal cell-derived factor-1α) ELISA kits (Boster, Wuhan, China) according to the manufacturer's protocols. Absorbance was measured with a microplate reader (Tecan Infinite 200, Mannedorf, Switzerland) at 450 nm. Moreover, paracrine of VEGF, SCF and SDF-1α in the peri-infarct region of the left ventricle (LV) was also examined using ELISA at 1 week after cell transplantation. In brief, LV tissues were cut into pieces and ground into tissue homogenate with homogenizer. After centrifugation, the supernatants were collected and stored at -20 ^{o}C. The cytokines were detected with ELISA kits. The experiment was repeated for thrice.

Detection of autophagy and apoptosis

To determine optimal preconditioning time of hypoxia and serum deprivation for c-kit$^+$VEGFR-2$^+$ MSCs, the degrees of autophagy and apoptosis of the cells were assessed with Western blotting and flow cytometry respectively. The cells were treated with hypoxia (1% O_2) and serum deprivation (3% FBS) for 1 hrs, 2 hrs, 4 hrs, 6 hrs and 8 hrs. After treatment, total protein in each group was extracted with RIPA buffer (Beyotime, Beijing, China) and separated in a 15% SDS-polyacrylamide gel. The lanes were

incubated with polyclone rabbit anti-rat LC3 (microtubule-associated protein 1 light chain 3) antibody (1:500; Novus, Littleton, CO, USA) and mouse anti-rat β-actin monoclonal antibody (1:4000; Proteintech, Rosemont, IL, USA) at 4 ^{o}C overnight. Then, they were incubated with anti-rabbit IgG HRP-linked antibody (1:4000; Cell Signaling, Danvers, MA, USA) and anti-mouse IgG HRP-linked antibody (1:4000; Cell Signaling) at room temperature for 1 hr. After being transferred onto a polyvinylidene fluoride membrane, the protein bands were monitored using Substrate Chemiluminescence Kit (Thermo, Rockford, IL, USA). The ratio of LC3-II/β-actin was analyzed using ImageJ (National Institutes of Health, Bethesda, MD, USA). The experiment was repeated for four times. For examining apoptosis of the hypoxia-treated cells, the cells were labeled with FITC Annexin V Apoptosis Detection Kit (BD Biosciences). The percentage of the apoptotic cells was determined by flow cytometry. The experiment was repeated for thrice.

Implantation of the cells into abdominal pouches

To assess the survival of the cells preconditioned with hypoxia and serum deprivation in the ischaemic tissue, the cells were implanted into abdominal subcutaneous pouches of SD rats. The pouches were prepared as previous method [29]. To mimic the ischaemic tissue, the subcutaneous vessels at the pouch were ligated. After treatment with 5 μM DiI for 20 min, the cells were suspended with 20 ng/mL fibrinogen and 50 IU/mL thrombin, and seeded on the poriferous polyethylene terephthalate membrane (pore size, 8 μm) removed from the transwell. For formation of fibrin gel, the cell-loaded membranes were incubated for 20 min. Then, the membranes were implanted into the abdominal pouches. At 24 hrs after implantation, the membranes were harvested, and the survived cells (DiI-labelled cells) were counted with a fluorescent microscope. Five fields of each membrane were selected randomly. The experiment was repeated for three times.

Scanning and transmission electron microscopies

The fibrin gel formed by mixing 500 μL of the fibrinogen (10 mg/mL) and 500 μL of thrombin (10 IU/mL; Sigma-Aldrich, St. Louis, MO, USA) in a 35-mm dish. The cells were seeded on the fibrin gel and incubated for 1 hr. Then, the specimens were pre-fixed with 1.25% glutaraldehyde and post-fixed with 1% buffered osmium tetroxide. After dehydration and substitution, the specimens were coated with gold-palladium and then viewed with a scanning electron microscope (Hitachi SU8010, Tokyo, Japan). In transmission electron microscopy, the specimens were fixed with 2.5% glutaraldehyde, post-fixed with 1% buffered osmium tetroxide and dehydrated with graded ethanol and acetone. The ultrathin sections were stained with uranyl acetate and lead citrate. The cells within the fibrin gel were viewed using a transmission electron microscope (CM120; Philips, Eindhoven, Holland). Moreover, compatibility of fibrin with the implanted cells and myocardium was examined by transmission electron microscopy at 2 hrs after transplantation.

Establishment of MI model and cell transplantation

Twenty-four adult female SD rats (200 ± 20 g) were anesthetized with ketamine (80 mg/kg) and xylazine (3 mg/kg). After endotracheal intubation, the heart was exposed, and the left anterior descending coronary artery (LAD) was ligated [30]. Two rats died immediately after LAD ligation. The rest rats were

divided into sham (n = 5), control (n = 5), cell (n = 6) and precondition (n = 6) groups. In control group, 40 μl fibrinogen (10 mg/ml) and 40 μl thrombin (10 IU/ml) were injected simultaneously with a Duploject syringe into the peri-infarcted region at four points. In the cell or precondition (1% O_2, 3% FBS) groups, 1 × 10^6 cells were suspended in fibrinogen.

Echocardiography

Echocardiograms were recorded with Vevo 2100 Imaging System (VisualSonics Inc., Toronto, ON, Canada) before MI, at 1 week after MI (before transplantation) and 4 weeks after transplantation respectively. The rats were anesthetized with isoflurane and fixed on the metal plate for detection. After adequate two-dimensional images had been obtained, the M-mode cursor was set to the parasternal long axis at the level of the papillary muscles. The LV end-diastolic diameter (LVEDD) and LV end-systolic diameter (LVESD) were measured from at least three consecutive cardiac cycles. To evaluate the systolic function, the LV end-diastolic volume (LVEDV), the LV end-systolic volume (LVESV), the ejection fraction (EF = LVEDV-LVESV/LVEDV×100%) and fractional shortening (FS = LVEDD − LVESD/LVEDD × 100%) were examined. Successful establishment of MI model was confirmed by EF of < 50% and FS of < 30%. Three measurements at least were taken and averaged for each parameter.

Masson’s trichrome staining

To evaluate myocardial repair of the infarcted region, the cryosections were performed with Masson’s trichrome. At 4 weeks after transplantation, the hearts were removed and perfused with 4% paraformaldehyde solution. Then, the hearts were cut into upper and lower parts along the cross-section, and continued to be fixed using 4% paraformaldehyde solution. After washing with DPBS, the tissue was treated with 16% and 30% sucrose gradient to dehydration, and then embedded with Tissue-Tek OCT (Sakura Finetek, Torrance, CA, USA). The cryosections (5-μm thickness) were prepared and stained. Scar tissue with plentiful collagen was stained blue, while myocardial tissue was stained red. The scar area was defined as percentage of circumference of infarct region in the whole LV wall circumference, and measured by Image J 1.46r (National Institutes of Health, Bethesda, MD, USA). The thickness of the LV wall at the infarcted region was measured at the thinnest part of the region. At least 5 independent sections and 2 fields (20 x) on each section were selected randomly.

Immunostaining of the myocardium

To determine angiogenesis of the peri-infarcted and infarcted regions, cryosections were incubated with mouse anti-rat CD31 antibody (1:200), followed by Alexa Fluor 594 conjugated goat anti-mouse IgG (1:400). Myocardial regeneration in the infarct region was assessed by double-labelled immunostaining using mouse anti-rat cTnT antibody (1:200) and rabbit anti-rat Cx43 antibody (1:100).

To trace differentiation of the transplanted cells into endothelial cells, smooth muscle cells and cardiomyocytes, the cells were labelled with GFP (green fluorescent protein) and co-localized with CD31, α-SMA and cTnT respectively. The gap junction between new cardiomyocytes differentiated from the transplanted cells and resident myocardium was determined by immunostaining of GFP, cTnT and Cx43.

The cryosections were incubated with chicken anti-rat GFP antibody (1:200; Novus), mouse anti-rat cTnT antibody (1:200) and rabbit anti-rat Cx43 antibody (1:100) overnight, followed with DyLight 488 goat anti-chicken IgG (H + L) (1:200; Novus), DyLight 594 goat anti-rabbit IgG (1:400; Abcam) and Alexa Fluor 647 goat anti-mouse IgG (1:400; ImmunoResearch Laboratories) respectively.

Statistical analysis

Data were presented as means ± standard deviation in the experiments above. Statistical analysis was conducted by SPSS 17.0 software (SPSS, Chicago, IL, USA) using t-test and one-way ANNOVA. $p < 0.05$ were regarded as the statistically significance.

Results

Phenotype and gene expression of c-kit $^{+}$ VEGFR-2 $^{+}$ MSCs

There was a population of c-kit^{+}VEGFR-2^{+} cells in MSCs isolated from bone marrow. MSCs highly expressed mesenchymal lineage markers (CD29, CD90 and CD105), and were negative for hematopoietic markers (CD34 and CD45) (Fig. 1A). The frequency of c-kit^{+}VEGFR-2^{+} cells sorted from MSCs was 5.07 ± 0.40% (Fig. 1B), about 70% of c-kit^{+} cells in MSCs. Fig. 1C showed immunostaining of c-kit^{+}VEGFR-2^{+} MSCs.

Gene expression profile revealed that there were 12491 genes in c-kit^{+}VEGFR2^{+} MSCs and 12231 genes in c-kit^{+}VEGFR2^{-} MSCs, which counted 71.59% and 70.10% as total gene numbers in Database respectively. Pearson's correlation coefficient values acrossing two samples was 0.91, which indicated a high consistence of whole genes in two samples (Fig. 2A). The volcano plot of all expressed genes was shown in Fig. 2B. Compared with expression of the genes in c-kit^{+}VEGFR2^{-} MSCs, c-kit^{+}VEGFR2^{+} MSCs contained 707 upregulated genes and 414 downregulated genes. Expression of most endothelium-specific genes (*Kdr*, *Vegfa*, *Angpt1*, *Ang*, *Flt4*, *Vegfc*, *Tie* and *Eng*) in c-kit^{+}VEGFR2^{+} MSCs was higher than that in c-kit^{+}VEGFR2^{-} MSCs, while expression of most smooth muscle-specific and myocardium-specific genes showed no significant difference between two populations of cells. Expression of mature endothelium-specific genes such as *Pecam1* and *vWF* was minimally observed in c-kit^{+}VEGFR2^{+} MSCs as well as c-kit^{+}VEGFR2^{-} MSCs, which coincided with stemness of MSCs (Fig. 2C). The 232 upregulated genes and 104 downregulated genes of c-kit^{+}VEGFR-2^{+} MSCs ($\log_2$FC > 1.5 or Log_2FC < -1.5 in all three experiments) were clustered respectively (Fig. 2D). Gene ontology analysis of the upregulated genes illustrated enrichment of genes related to immune process, cell migration, cell differentiation, angiogenesis (*Itgb2*, *Pf4*, *C5ar1*, *Chi3l1*, *Camp*, *Mmp9*, *Kdr*, *Enpp2*, *C3*, *Efna1* and *Adm*), VEGF production and cardiovascular system development (*Angpt1*, *Angptl4*, *Hpse*, *Tgfbr3*, *Cdh2*, *Nox1*, *Spil*, *Kdr*, *Adm*, *Ccl12*, *Pdpn*, *Apln*, and *Efna1*). Some typical pathways reflecting cell function such as blood vessel morphogenesis and cytokine production were overrepresented significantly among the upregulated genes in c-kit^{+}VEGFR-2^{+} MSCs (Fig. 2E), and their first neighbor network construction was demonstrated in Fig,

S1. KEGG pathway analysis confirmed that the upregulated genes were enriched in VEGF, HIF and chemokine signaling pathways, which showed the superiority of the cells in cytokine secretion and vascular formation. Moreover, in terms of metabolism, the up-regulated genes were also enriched in biosynthesis of amino acids and glycolysis, which indicated that c-kit^{+}VEGFR2^{+} MSCs possess high tolerance to hypoxia than c-kit^{+}VEGFR2^{-} MSCs (Fig. 2F).

Properties of c-kit $^{+}$ VEGFR-2 $^{+}$ MSCs

After treatment with VEGF and SCF, the proliferated cells and migrated cells were increased significantly. The numbers of the proliferated cells and migrated cells in the VEGF + SCF group were greater than the VEGF group or SCF group (Fig. 3A, B). Compared with the control group, more c-kit^{+}VEGFR2^{+} MSCs incorporated to the capillary-like structures formed by the endothelial cells in the VEGF group (Fig. 3C, D).

The results of RT-PCR and immunostaining demonstrated that c-kit^{+}VEGFR2^{+} MSCs differentiated into endothelial cells, smooth muscle cells and myocardiocytes after induction for 2 weeks. After VEGF induction, the cells expressed CD31 and vWF and demonstrated a typical cobblestone appearance like endothelial cells (Fig. 4A–D). With TGF-β induction, the cells expressed *α-SMA* and *CNN1* and were positive for α-SMA and desmin immunostaining (Fig. 4E through G). BMP-2-induced cells expressed *NKX2.5* and *GATA-4* and were positive for cTnT immunostaining. The cells represented a morphological feature of parallel alignment. Cx43 was granular and located at the conjunctions of the cells (Fig. 4H–K).

Optimal preconditioning of hypoxia and serum deprivation

After treatment with hypoxia (1% O_2) and serum deprivation (3% FBS), the number of the apoptotic cells constantly increased. Ratio of LC3-II/β-actin reached the plateau at 4 hrs after treatment. According to the balance of autophagy and apoptosis, the level of autophagy was near to the plateau at 4 hrs after treatment, while the degree of apoptosis was not much high at this time point (Fig. 5A–E). Therefore, 4 hrs was regarded as an optimal preconditioning time for c-kit^{+}VEGFR-2^{+} MSC transplantation. In the abdominal ischaemic pouch assay, the number of the survived cells in the cells preconditioned with hypoxia and serum deprivation for 4 hrs was greater than control group (Fig. 5F–G). This result shows that preconditioning is effective for improving survival of the transplanted cells.

After treatment with hypoxia for 12 hrs, concentrations of VEFG, SCF and SDF-1α secreted from c-kit^{+}VEGFR-2^{+} MSCs were increased significantly (Fig. 5H).

Compatibility of fibrin with the implanted cells and myocardium

In the images of scanning electron microscope, fibrin constituted a delicate fibrous network, and the cells spread well on the network (Fig. S2A, B). In the images of transmission electron microscope, the cells

grew well in the fibrin gel (Fig. S2C). Fibrin represents a good compatibility with the implanted cells and myocardium (Fig. S2D, E).

Improvement of cardiac function after cell transplantation

Representative echocardiograms of the LV free walls were shown in Fig. 6A. The echocardiograms revealed that cardiac function in all mice was severely compromised at 1 week after MI. In the control group, the loss of cardiac function lasted for 4 weeks. At 4 weeks after transplantation of c-kit$^+$VEGFR-2$^+$ MSCs, LV contraction in the cell and precondition groups was significantly improved. Compared with the cell group, LV contraction in the precondition group was strengthened significantly. After transplantation, the EF and FS were increased in the cell group and precondition group, while the precondition group showed a remarkably greater EF and FS than cell group (Fig. 6B, C).

Histological changes of the LV wall after transplantation

The morphological changes of the LV wall were shown in Fig. 6D. In the control group, the myocardium of the infarcted region was replaced by fibrous tissue at 4 weeks post-MI. There was more myocardium at the infarcted region in the cell and precondition groups at 4 weeks after cell transplantation. The thickness of the LV wall in the precondition group was greater than the cell group. The scar size was decreased after transplantation. The scar size in the precondition group was significantly smaller than the cell group (Fig. 6E, F).

Differentiation of the engrafted cells

At 4 weeks after transplantation, some the engrafted cells (GFP$^+$ cells) expressed CD31, α-SMA or cTnT. GFP$^+$CD31$^+$ cells and GFP$^+$α-SMA$^+$ cells were observed to be incorporated to the wall of the microvessels. GFP$^+$cTnT$^+$ cells were parallel with native cardiomyocytes (Fig. 7A–C). Cx43 expression was found to be located at conjunction of GFP$^+$cTnT$^+$ cell and native cardiomyocyte (Fig. 7D).

Enhancement of paracrine in the peri-infarcted myocardium after transplantation

At 1 week after transplantation, concentrations of VEFG, SCF and SDF-1α in plasma in the precondition group was higher than that in cell group. Compared with the control group, concentration of SDF-1α in the cell group was higher. Difference in concentrations of VEFG and SCF between the cell group and control group was not significant. In the peri-infarcted myocardium, concentrations of these cytokines in the cell group were higher than that in the control group. Compared with the cell group, concentrations of these cytokines in the precondition group were higher (Fig. S3).

Angiogenesis and myocardium regeneration after transplantation

After transplantation for 4 weeks, angiogenesis in both infarcted and peri-infarcted regions was assessed by counting the number of CD31$^+$ microvessels. There were more microvessels in the cell and

precondition groups. The density of the microvessels in the precondition group was significantly greater than that in the cell group (Fig. 8A–C). In addition to the cardiomyocytes differentiated from the engrafted cells, myocardial regeneration at the infarct region was evaluated by immunostaining of cTnT and Cx43 at 4 weeks after transplantation. Compared with control group, the myocardium and $Cx43^+$ conjunctions of cardiomyocytes were increased significantly at the infarcted region in the cell group and precondition groups, while more regenerated myocardium was observed in the precondition group (Fig. 8D).

Discussion

In this study, we found that there is population of c-kit^+VEGFR-2^+ cells in bone marrow-derived MSCs. The number of the VEGFR-2^+ cells is 70% in c-kit^+ MSCs. This study highlights the heterogeneity of c-kit MSCs. c-kit^+VEGFR-2^+ MSCs have a potential to differentiate towards endothelial cells, smooth muscle cells and cardiomyocytes. c-kit^+VEGFR-2^+ MSCs express most smooth muscle-specific and myocardium-specific genes, while endothelium-specific genes are highly expressed. The upregulated genes are involved in immune response, cell migration, cell differentiation, and angiogenesis. Transplantation of c-kit^+VEGFR-2^+ MSCs is effective in improving cardiac function and alleviating adverse ventricular remodeling post-MI. The transplanted cells can incorporate to the microvessels for participating in angiogenesis. Moreover, the differentiated cells can conjunct with native cardiomyocytes to form the functional myocardium. These results suggest that c-kit^+VEGFR-2^+ MSCs are a novel population of stem cells for MI therapy. This study and other studies [31] show that VEGFR-2 signalling plays a vital role in diffferentiation of stem/progenitor cells into endothelial cells. Therefore, transplantation of c-kit^+VEGFR-2^+ MSCs may be used to promote angiogenesis in other ischaemic diseases such as critical limb ischaemia in diabetes. Further study is needed to investigate cardiomyogenic potential and therapeutic effects of c-kit^+VEGFR-2^- MSCs.

The results of this study demonstrate that paracrine of c-kit^+VEGFR-2^+ MSCs enhance engraftment of c-kit^+VEGFR-2^+ MSCs in the ischaemic myocardium. In the condition of hypoxia, secretion of VEGF, SCF and SDF-1α by c-kit^+VEGFR-2^+ MSCs is increased. In recent years, attention has been paid on paracrine mechanisms of reparative and regenerative effects of stem cells [32]. Clinical trials have suggested that secretion of paracrine factors may be the underlying mechanism responsible for the improvement in outcomes [33]. Both VEGF and SCF promote proliferation and migration of c-kit^+VEGFR-2^+ MSCs, while the effects of VEGF and SCF are synergetic. VEGF activates incorporation of c-kit^+VEGFR-2^+ MSCs to the microvessels. Moreover, SCF may induce recruitment and expansion of c-kit^+ cells [34]. Expression of c-kit in CSCs is upregulated in response to pathological stress. Activation of c-kit receptor mediates cell survival and proliferation of stem cells [35]. Taken together, SCF/c-kit and VEGF/VEGFR-2 signalling pathways regulate the activities of c-kit^+VEGFR-2^+ MSCs. In addition, SDF-1α-CXCR4 axis plays a crucial

role in homing of stem or progenitor cells from bone marrow to ischaemic myocardium [36]. MSCs can stimulate CSC chemotaxis via SDF-1α/CXCR4 signalling pathway [37]. The recent study shows that paracrine of the engrafted MSCs account for activation the epicardium and recruitment of endogenous stem cells [30]. Thus, effects of paracrine of c-kit$^+$VEGFR-2$^+$ MSCs on endogenous repair of the infarct myocardium are deserved to be explored.

Survival and differentiation of the engrafted cells within hostile ischaemic and inflammatory microenvironment are poor [38]. Our experimental data reveal that preconditioning with hypoxia and serum deprivation may be beneficial for survival and differentiation of the transplanted c-kit$^+$VEGFR-2$^+$ MSCs. According to balance of autophagy and apoptosis induced with hypoxia and serum deprivation, treatment with 1% O_2 and 3% FBS for 4 hrs was determined as optimal preconditioning of c-kit$^+$VEGFR-2$^+$ MSCs. Moderate rapamycin-primed MSCs can promote repair of the infarcted myocardium after transplantation [39]. Hypoxia-activated autophagy augments survival of endothelial progenitor cells by inhibiting apoptosis [40]. Hypoxia-preconditioned endothelial progenitor cells promote repair of the ischaemic hindlimb after transplantation [29]. Contribution of autophagy to preconditioning with hypoxia and serum deprivation enhances adaptation of the transplanted c-kit$^+$VEGFR-2$^+$ MSCs to ischaemic microenvironment. Moreover, we found fibrin is reliable in delivery of c-kit$^+$VEGFR-2$^+$ MSCs. Fibrin has cytoprotection in the condition of hypoxia, and represents good compatibility with the implanted cells and myocardium. Infarction of myocardium leads to degradation of extracellular matrix, which influences the regenerative capability of the myocardium [41]. Fibrin favors to retention and survival of the transplanted c-kit$^+$VEGFR-2$^+$ MSCs.

Conclusion

This study suggests that bone marrow-derived c-kit$^+$VEGFR-2$^+$ MSCs have a potential to differentiate towards cardiovascular cells. The cells can effectively repair the infarcted myocardium after transplantation. Differentiation as well as paracrine of the cells contributes to myocardiac regeneration. Moreover, this study provides a feasible approach to activate autophagy with preconditioning with hypoxia and serum deprivation. We propose that application of reliable stem cells and optimal strategies of transplantation may enhance efficiency of stem cell therapy for MI.

Abbreviations

BMP-2: Bone morphogenetic protein-2; CNN1: Calponin 1; CSC: Cardiac stem cell; cTnT: Cardiac troponin T; Cx43: Connexin-43; DMEM: Dulbecco's modified Eagle's medium; EDTA: Ethylene diamine tetraacetic acid; EF: Ejection fraction; ELISA: Enzyme-linked immunosorbent assay; FBS: Fetal bovine serum; FS: Fractional shortening; *GFP*: Green fluorescent protein; GO: Gene ontology; KEGG: Kyoto Encyclopedia of Genes and Genomes; LAD: Left anterior descending coronary artery; LC3: Microtubule-associated protein 1 light chain 3; LV: Left ventricle; LVEDD: LV end-diastolic diameter; LVEDV: LV end-diastolic volume; LVESD: LV end-systolic diameter; LVESV: LV end-systolic volume; MI: Myocardial infarction; MSC:

Mesenchymal stem cell; RT-PCR: Reverse transcription-polymerase chain reaction; SCF: Stem cell factor; SD: Sprague-Dawley; SDF-1α: Stromal cell-derived factor-1α; TGF-β: Transforming growth factor-β; VEGF: Vascular endothelial growth factor; VEGFR-2: Vascular endothelial growth factor receptor-2; vWF: von Willebrand factor; α-SMA: α-smooth muscle actin.

Declarations

Acknowledgements

Not applicable.

Authors' contributions

H-JW and Y-ZT conceived and designed the experiments. PZ, H-FZ, Y-LW, and PT performed the experiments. PZ and H-FZ analyzed and interpreted the data. H-JW, PZ and Y-ZT wrote the paper. All authors read and approved the final manuscript.

Funding

This work was supported by National Natural Science Foundation of China (81470385 and 81770288 to YZT, 81870215 to HJW) and Specialized Research Fund for the Doctoral Program of Higher Education (20130071110080 to HJW).

Availability of data and materials

The original data are available from the corresponding author on request.

Ethics approval and consent to participate

This study was approved by Institutional Animal Care Committee of Fudan University (SYXK 2009-0082).

Consent for publication

Not applicable.

Competing interests

The authors declare that they have no competing interests.

Author details

Department of Anatomy, Histology and Embryology, Shanghai Medical School of Fudan University, Shanghai 200032, China

References

1. Mozaffarian D, Benjamin EJ, Go AS, et al. Heart disease and stroke statistics-2016 update: a report from the American Heart Association. Circulation. 2016;133:e38–60.
2. McDonagh TA, Metra M, Adamo M, et al. 2021 ESC Guidelines for the diagnosis and treatment of acute and chronic heart failure: Developed by the Task Force for the diagnosis and treatment of acute and chronic heart failure of the European Society of Cardiology (ESC) with the special contribution of the Heart Failure Association (HFA) of the ESC. Eur Heart J. 2021;42:3599–726.
3. Murry CE, Reinecke H, Pabon LM. Regeneration gaps: observations on stem cells and cardiac repair. J Am Coll Cardiol. 2006;47:1777–85.
4. Laflamme MA, Murry CE. Heart regeneration. Nature. 2011;473:326–35.
5. Bergmann O, Bhardwaj RD, Bernard S, Zdunek S, Barnabe-Heider F, Walsh S, Zupicich J, Alkass K, Buchholz BA, Druid H, Jovinge S, Frisen J. Evidence for cardiomyocyte renewal in humans. Science. 2009;324:98–102.
6. Young PP, Schafer R. Cell-based therapies for cardiac disease: a cellular therapist's perspective. Transfusion. 2015;55:441–51.
7. Tompkins BA, Balkan W, Winkler J, Gyöngyösi M, Goliasch G, Fernández-Avilés F, Hare JM. Preclinical studies of stem cell therapy for heart disease. Circ Res. 2018;122:1006–20.
8. Gude NA, Sussman MA. Cardiac regenerative therapy: Many paths to repair. Trends Cardiovas Med. 2020;30:338–43.
9. Li M, Naqvi N, Yahiro E, Liu K, Powell PC, Bradley WE, Martin DIK, Graham RM, Dell'Italia LJ, Husain A. c-kit is required for cardiomyocyte terminal differentiation. Circ Res. 2008;102:677–85.
10. Wu SM, Fujiwara Y, Cibulsky SM, Clapham DE, Lien CL, Schultheiss TM, Orkin SH. Developmental origin of a bipotential myocardial and smooth muscle cell precursor in the mammalian heart. Cell. 2006;127:1137–50.
11. Beltrami AP, Barlucchi L, Torella D, Baker M, Limana F, Chimenti S, Kasahara H, Rota M, Musso E, Urbanek K, Leri A, Kajstura J, Nadal-Ginard B, Anversa P. Adult cardiac stem cells are multipotent and support myocardial regeneration. Cell. 2003;114:763–76.

12. Bearzi C, Rota M, Hosoda T, Tillmanns J, Nascimbene A, De Angelis A, Yasuzawa-Amano S, Trofimova I, Siggins RW, Lecapitaine N, Cascapera S, Beltrami AP, D'Alessandro DA, Zias E, Quaini F, Urbanek K, Michler RE, Bolli R, Kajstura J, Leri A, Anversa P. Human cardiac stem cells. Proc Natl Acad Sci USA. 2007;104:14068–73.
13. Ellison GM, Vicinanza C, Smith AJ, Aquila I, Leone A, Waring CD, Henning BJ, Stirparo GG, Papait R, Scarfò M, Agosti V, Viglietto G, Condorelli G, Indolfi C, Ottolenghi S, Torella D, Nadal-Ginard B. Adult c-kit^{pos} cardiac stem cells are necessary and sufficient for functional cardiac regeneration and repair. Cell. 2013;154:827–42.
14. Zaruba M-M, Soonpaa M, Reuter S, Field LJ. Cardiomyogenic potential of C-kit+-expressing cells derived from neonatal and adult mouse hearts. Circulation. 2010;121:1992–2000.
15. Elhelaly WM, Cardoso AC, Pereira AHM, Elnawasany A, Ebrahimi S, Nakada Y, Sadek HA. C-Kit cells do not significantly contribute to cardiomyogenesis during neonatal heart regeneration. Circulation. 2019;139:559–61.
16. van Berlo JH, Kanisicak O, Maillet M, Vagnozzi RJ, Karch J, Lin SC, Middleton RC, Marbán E, Molkentin JD. c-kit^{+} cells minimally contribute cardiomyocytes to the heart. Nature. 2014;509:337–41.
17. Vicinanza C, Aquila I, Scalise M, Cristiano F, Marino F, Cianflone E, Mancuso T, Marotta P, Sacco W, Lewis FC, Couch L, Shone V, Gritti G, Torella A, Smith AJ, Terracciano CM, Britti D, Veltri P, Indolfi C, Nadal-Ginard B, Ellison-Hughes GM, Torella D. Adult cardiac stem cells are multipotent and robustly myogenic: c-kit expression is necessary but not sufficient for their identification. Cell Death Differ. 2017;24:2101–16.
18. Huang E, Nocka K, Beier DR, Chu TY, Buck J, Lahm HW, Wellner D, Leder P, Besmer P. The hematopoietic growth factor KL is encoded by the Sl locus and is the ligand of the c-kit receptor, the gene product of the W locus. Cell. 1990;63:225–33.
19. Murry CE, Soonpaa MH, Reinecke H, Nakajima H, Nakajima HO, Rubart M, Pasumarthi KB, Virag JI, Bartelmez SH, Poppa V, Bradford G, Dowell JD, Williams DA, Field LJ. Haematopoietic stem cells do not transdifferentiate into cardiac myocytes in myocardial infarcts. Nature. 2004;428:664–8.
20. Karantalis V, Hare JM. Use of mesenchymal stem cells for therapy of cardiac disease. Circ Res. 2015;116:1413–30.
21. Cashman TJ, Gouon-Evans V, Costa KD. Mesenchymal stem cells for cardiac therapy: practical challenges and potential mechanisms. Stem Cell Rev Rep. 2013;9:254–65.
22. Attar A, Bahmanzadegan Jahromi F, Kavousi S, Monabati A, Kazemi A. Mesenchymal stem cell transplantation after acute myocardial infarction: a meta-analysis of clinical trials. Stem Cell Res Ther. 2021;12:600.
23. Orlic D, Kajstura J, Chimenti S, Jakoniuk I, Anderson SM, Li B, Pickel J, McKay R, Nadal-Ginard B, Bodine DM, Leri A, Anversa P. Bone marrow cells regenerate infarcted myocardium. Nature. 2001;410:701–5.

24. Taghavi S, Sharp TE III, Duran JM, Makarewich CA, Berretta RM, Starosta T, Kubo H, Barbe M, Houser SR. Autologous c-Kit+ mesenchymal stem cell injections provide superior therapeutic benefit as compared to c-Kit+ cardiac-derived stem cells in a feline model of isoproterenol-induced cardiomyopathy. Clin Trans Sci. 2015;8:425–31.
25. Wang YL, Zhang GT, Wang HJ, Tan YZ, Wang XY. Preinduction with bone morphogenetic protein-2 enhances cardiomyogenic differentiation of c-kit$^+$ mesenchymal stem cells and repair of infarcted myocardium. Int J Cardiol. 2018;265:173–80.
26. Zhang DY, Wang HJ, Tan YZ. Wnt/beta-catenin signaling induces the aging of mesenchymal stem cells through the DNA damage response and the p53/p21 pathway. PLoS One. 2011;6:e21397.
27. Wang YL, Yu SN, Shen HR, Wang HJ, Wu XP, Wang QL, Zhou B, Tan YZ. Thymosin β4 released from functionalized self-assembling peptide activates epicardium and enhances repair of infarcted myocardium. Theranostics. 2021;11:4262–80.
28. Zhang HF, Wang YL, Tan YZ, Wang HJ, Tao P, Zhou P. Enhancement of cardiac lymphangiogenesis by transplantation of CD34$^+$VEGFR-3$^+$ endothelial progenitor cells and sustained release of VEGF-C. Basic Res Cardiol. 2019;114:43.
29. Zhou P, Tan YZ, Wang HJ, Wang GD. Hypoxic preconditioning-induced autophagy enhances survival of engrafted endothelial progenitor cells in ischaemic limb. J Cell Mol Med. 2017;21:2452–64.
30. Wang QL, Wang HJ, Li ZH, Wang YL, Wu XP, Tan YZ. Mesenchymal stem cell-loaded cardiac patch promotes epicardial activation and repair of the infarcted myocardium. J Cell Mol Med. 2017;21:1751–66.
31. Cooke JP, Losordo DW. Modulating the vascular response to limb ischemia: angiogenic and cell therapies. Circ Res. 2015;116:1561–78.
32. Hodgkinson CP, Bareja A, Gomez JA, Dzau VJ. Emerging concepts in paracrine mechanisms in regenerative cardiovascular medicine and biology. Circ Res. 2016;118:95–107.
33. Madonna R, Ferdinandy P, De Caterina R, Willerson JT, Marian AJ. Recent developments in cardiovascular stem cells. Circ Res. 2014;115:e71–8.
34. Yaniz-Galende E, Chen J, Chemaly E, Liang L, Hulot J-S, McCollum L, Arias T, Fuster V, Zsebo KM, Hajjar RJ. Stem cell factor gene transfer promotes cardiac repair after myocardial infarction via in situ recruitment and expansion of c-kit$^+$ cells. Circ Res. 2012;111:1434–45.
35. Gude NA, Firouzi F, Broughton KM, Ilves K, Nguyen KP, Payne CR, Sacchi V, Monsanto MM, Casillas AR, Khalafalla FG, Wang BJ, Ebeid DE, Alvarez R, Dembitsky WP, Bailey BA, van Berlo J, Sussman MA. Cardiac c-Kit biology revealed by inducible transgenesis. Circ Res. 2018;123:57–72.
36. Ziff OJ, Bromage DI, Yellon DM, Davidson SM. Therapeutic strategies utilizing SDF-1α in ischaemic cardiomyopathy. Cardiovas Res. 2018;114:358–67.
37. Hatzistergos KE, Saur D, Seidler B, Balkan W, Breton M, Valasaki K, Takeuchi LM, Landin AM, Khan A, Hare JM. Stimulatory effects of mesenchymal stem cells on cKit$^+$ cardiac stem cells are mediated by SDF1/CXCR4 and SCF/cKit signaling pathways. Circ Res. 2016;119:921–30.

38. Behfar A, Crespo-Diaz R, Terzic A, Gersh BJ. Cell therapy for cardiac repair–lessons from clinical trials. Nat Rev Cardiol. 2014;11:232–46.
39. Li ZH, Wang YL, Wang HJ, Wu JH, Tan YZ. Rapamycin-preactivated autophagy enhances survival and differentiation of mesenchymal stem cells after transplantation into infarcted myocardium. Stem Cell Rev Rep. 2020;16:344–56.
40. Wang HJ, Zhang D, Tan YZ, Li T. Autophagy in endothelial progenitor cells is cytoprotective in hypoxic conditions. Am J Physiol Cell Physiol. 2013;304:C617–26.
41. Grigorian Shamagian L, Madonna R, Taylor D, Climent AM, Prosper F, Bras-Rosario L, Bayes-Genis A, Ferdinandy P, Fernández-Avilés F, Izpisua Belmonte JC, Fuster V, Bolli R. Perspectives on directions and priorities for future preclinical studies in regenerative medicine. Circ Res. 2019;124:938–51.

Figures

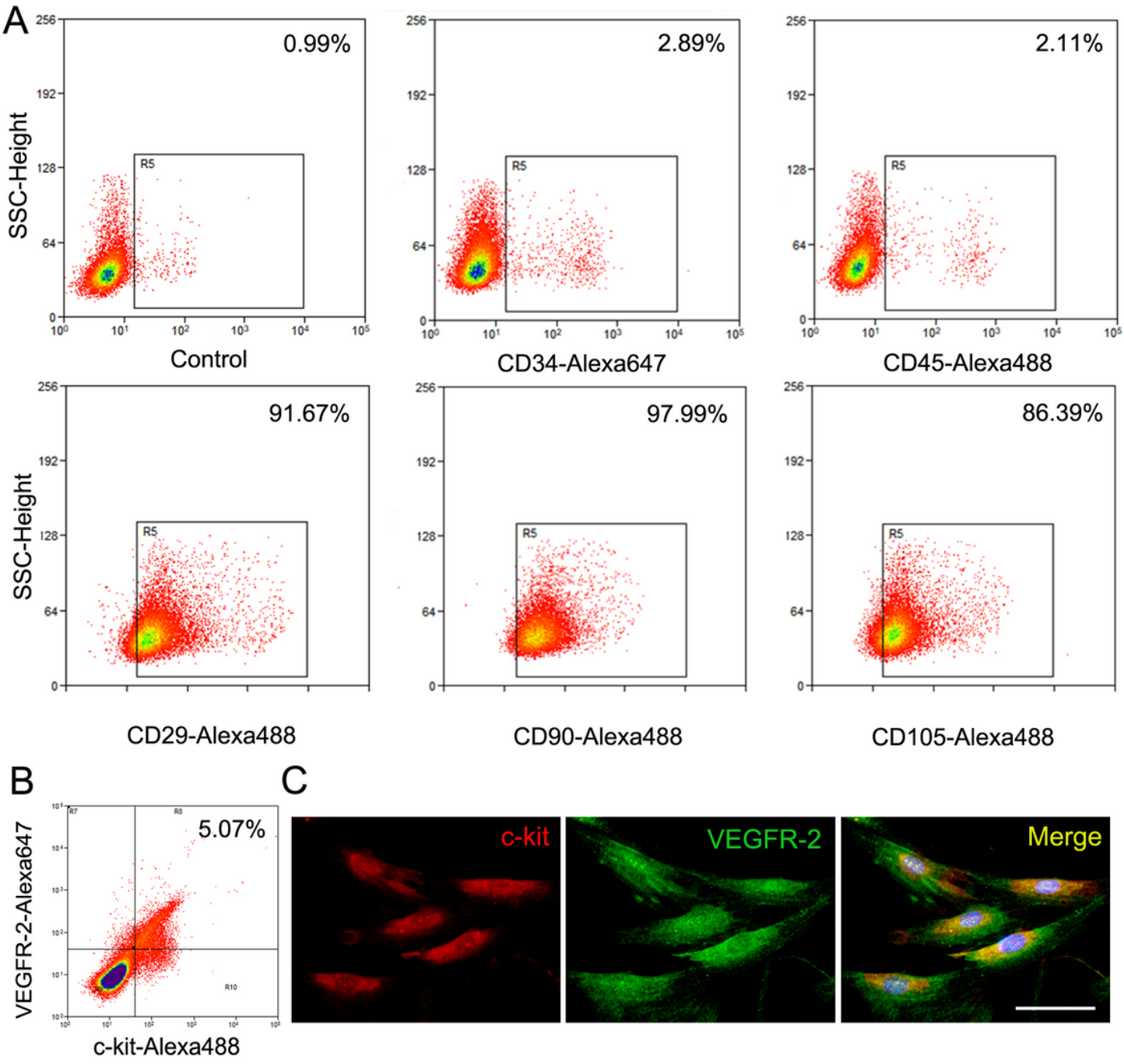

Figure 1

Characterization of c-kit$^+$VEGFR-2$^+$ MSCs. **A** The flow cytometric analysis of CD34$^+$, CD45$^+$, CD29$^+$, CD90$^+$ or CD105$^+$ cells in MSCs isolated from the mononuclear cells of rat bone marrow. **B** The phenotype of MSCs analyzed by dual-color flow cytometry. Percentage of the positive cells was compared to isotype control. **C** The sorted c-kit$^+$VEGFR-2$^+$ MSCs. Immunostaining. Scale bar=50 μm.

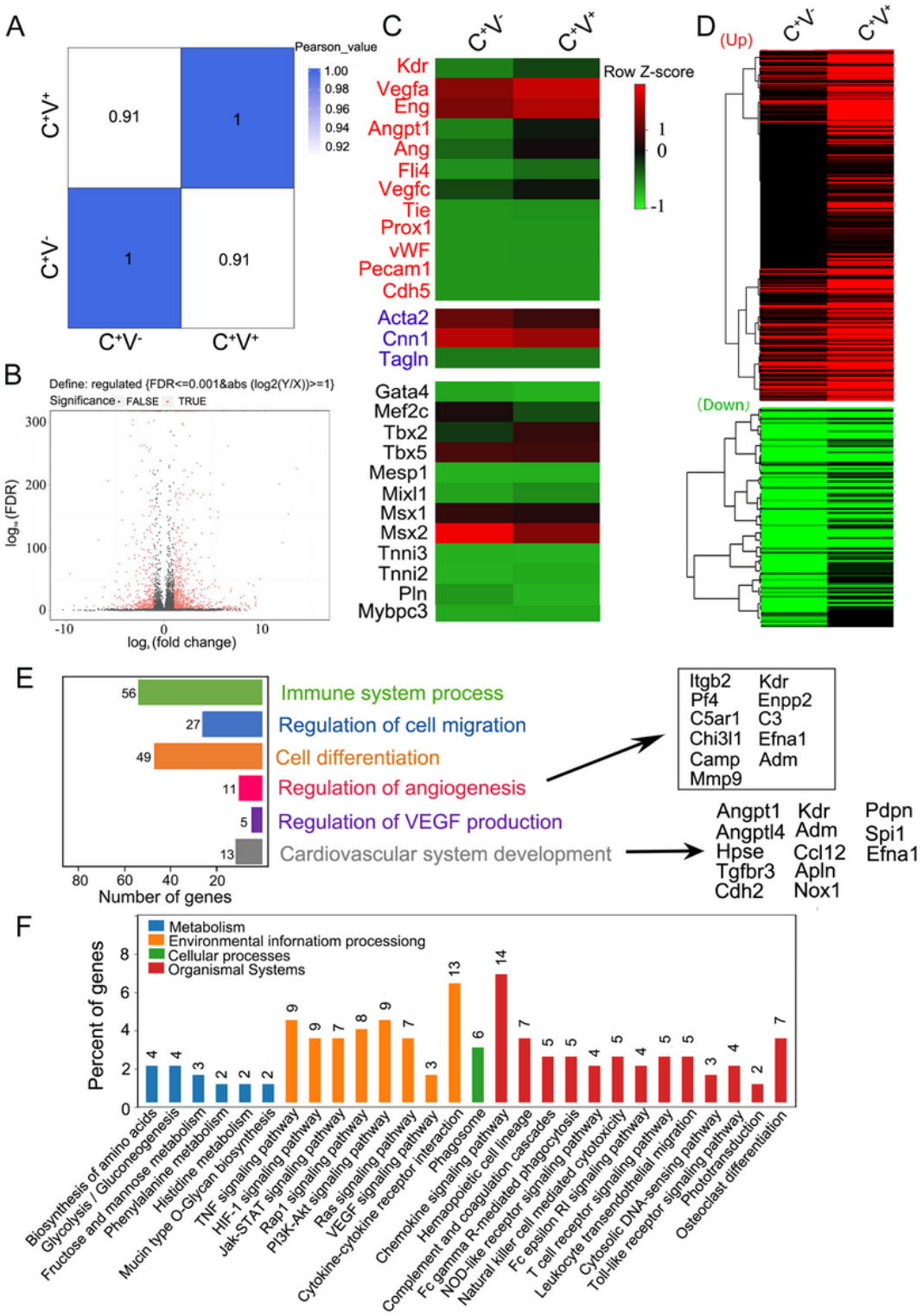

Figure 2

Gene expression profile of c-kit^{+}VEGFR-2^{+} MSCs. **A** Pearson's correlation coefficient of C^{+}V^{-} and C^{+}V^{+}groups. C^{+}V^{-}, c-kit^{+}VEGFR-2^{-} MSCs; C^{+}V^{+}, c-kit^{+}VEGFR-2^{+} MSCs. **B** Volcano plot of all expressed genes. **C** Dynamic expression of cardiovascular lineage genes. Types of markers were color-coded in heat map. Red, endothelial cell markers; blue, smooth muscle cell markers; black, cardiomyocyte markers. **D** Hierarchical clustering of the significantly unregulated genes and downregulated genes. **E** Gene ontology

analysis of the upregulated genes. **F** KEGG pathway analysis of biological processes based on the upregulated genes.

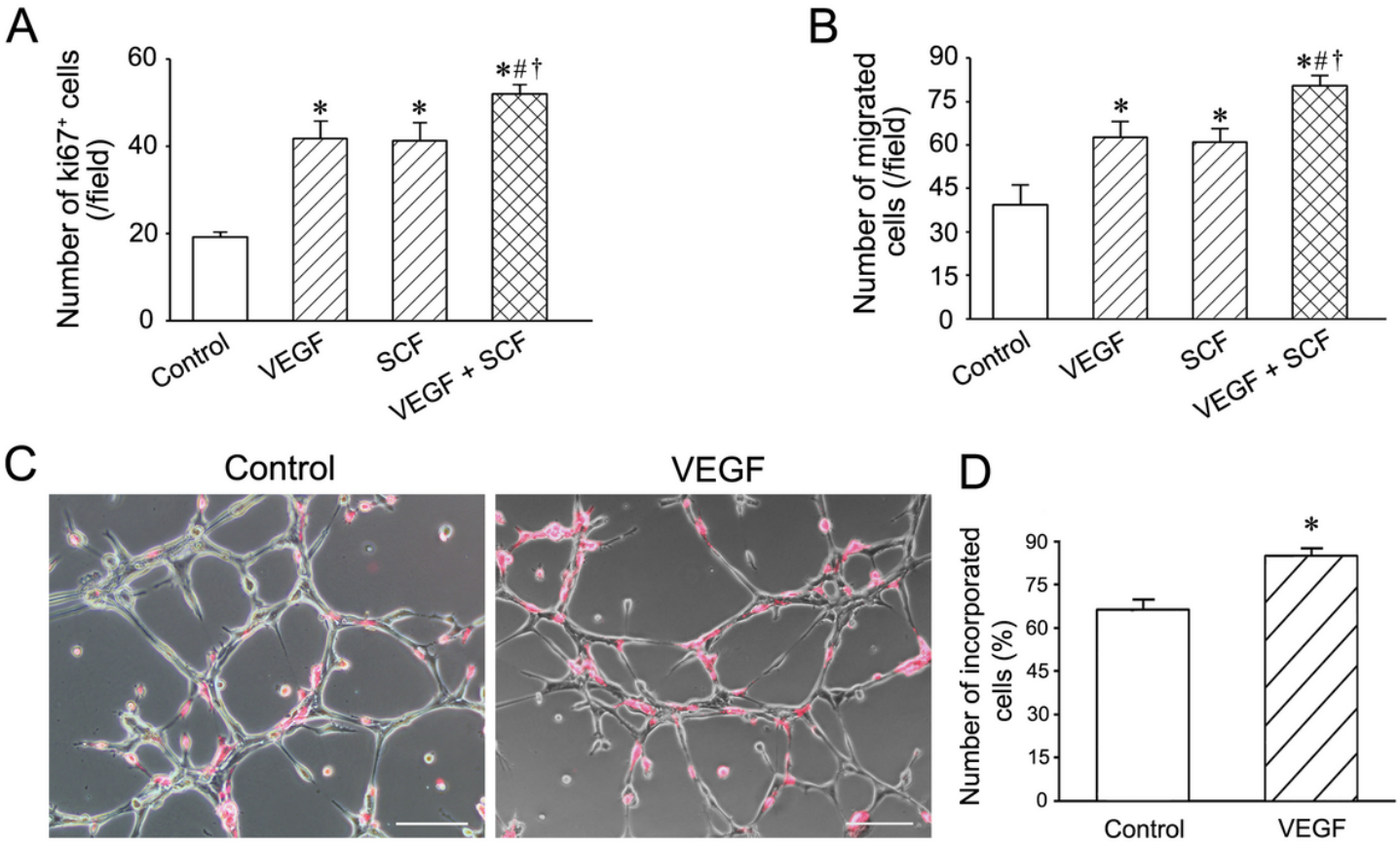

Figure 3

Proliferation, migration and incorporation of c-kit$^+$VEGFR-2$^+$ MSCs. **A** Effects of VEGF and SCF on proliferation of the cells. **B** Effects of VEGF and SCF on migration of the cells. *$p < 0.05$ versus control group, #$p < 0.05$ versus VEGF group, †$p < 0.05$ versus SCF group. n=6. **C** Incorporation of c-kit$^+$VEGFR-2$^+$ MSCs to the capillary-like structures formed by pulmonary microvascular endothelial cells. c-kit$^+$VEGFR-2$^+$ MSCs were labelled with Dil. Scar bar=100 μm. **D** The statistical result of the incorporated c-kit$^+$VEGFR-2$^+$ MSCs after VEGF induction. *$p < 0.05$ versus control group. n=4.

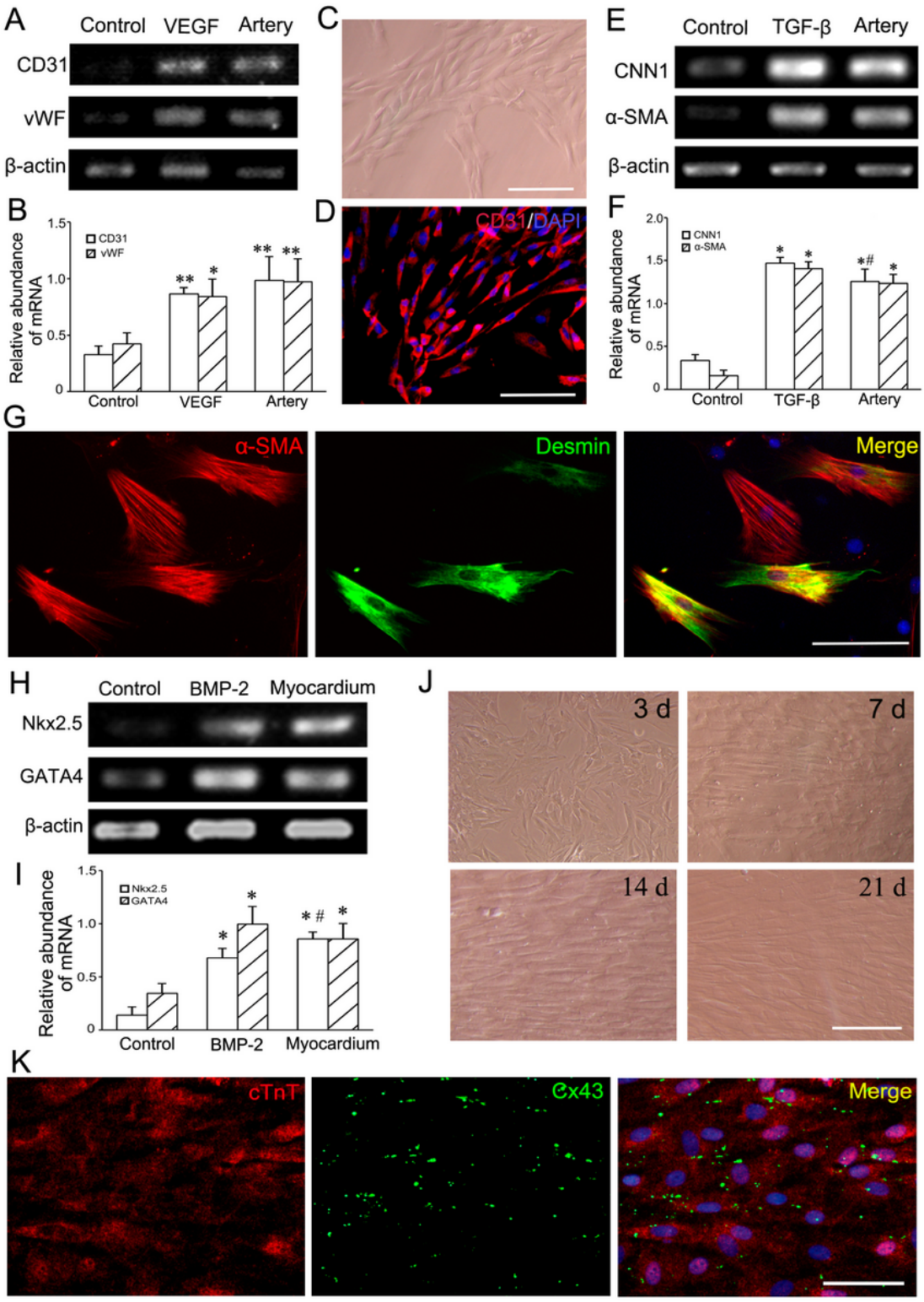

Figure 4

Differentiation of c-kit^{+}VEGFR-2^{+} MSCs into cardiovascular cells after induction for two weeks. **A** Expression of CD31 and vWF mRNAs in the VEGF-induced cells. **B** Statistical result of expression of CD31 and vWF mRNAs. *p < 0.05, **p < 0.01 versus control group. n=3. **C** The phase contrast image of the VEGF-induced cells. **D** CD31 immunostaining of the differentiated cells. **E** Expression of CNN1 and α-SMA mRNAs in the TGF-β-induced cells. **F** The statistical result of expression of CNN1 and α-SMA mRNAs. *p <

0.05 versus control group, #$p < 0.05$ versus TGF-β group. The femoral artery from SD rat as positive control. n=3. **G** Immunostaining of α-SMA and desmin in the differentiated cells. **H** Expression of Nkx2.5 and GATA4 mRNAs in the BMP-2-induced cells. **I** The statistical result of expression of Nkx2.5 and GATA4 mRNAs. The myocardium from SD rat as positive control. *$p < 0.05$ versus control group, #$p < 0.05$ versus BMP-2 group. n=3. **J** The phase contrast images of the cells at 3, 7, 14 and 21 days after BMP-2 induction. **K** Immunostaining of cTnT and Cx43 in the differentiated cells. Scale bar=100 μm.

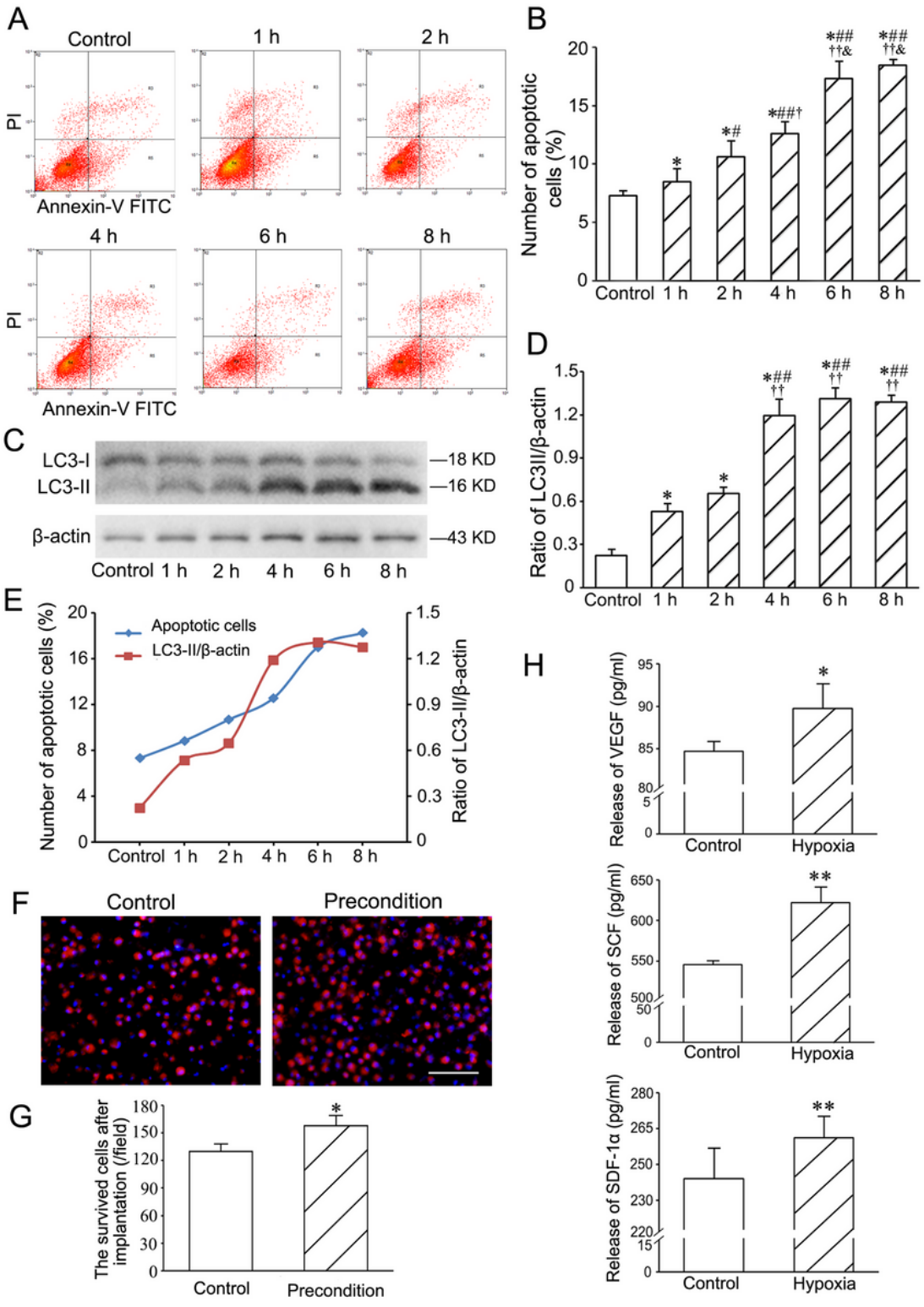

Figure 5

Determination of the optimal preconditioning of hypoxia and serum deprivation for c-kit^{+}VEGFR-2^{+} MSCs. **A** The typical quadrantal diagrams of flow cytometric analysis of the apoptotic cells. The cells were treated with 1% O_2 and 3% FBS. **B** The statistic result of the numbers of the apoptotic cells. *$p < 0.05$ versus control group, #$p < 0.05$ and ##$p < 0.01$ versus 1 h group, †$p < 0.05$ and ††$p < 0.01$ versus 2 h group, & $p < 0.05$ versus 4 h group. n=3. **C** Western blotting of LC3 in the cells. **D** The statistic result of LC3II/β-actin ratios. *$p < 0.05$ versus control group, ##$p < 0.01$ versus 1 h group, ††$p < 0.01$ versus 2 h group. n=4. **E** The curves of the numbers of the apoptotic cells and LC3-II/β-actin ratios. **F** The survived cells in the cells preconditioned with hypoxia and serum deprivation for 4 hrs after implantation into the abdominal ischaemic pouch. Scale bar=100 μm. **G** The statistical result of the numbers of the survived cells. *$p < 0.05$ versus control group. n=6. **H** Concentration of VEGF, SCF and SDF-1α from the cells treated with hypoxia (1% O_2) for 12 hrs. *$p < 0.05$, **$p < 0.01$ versus control group. n=6.

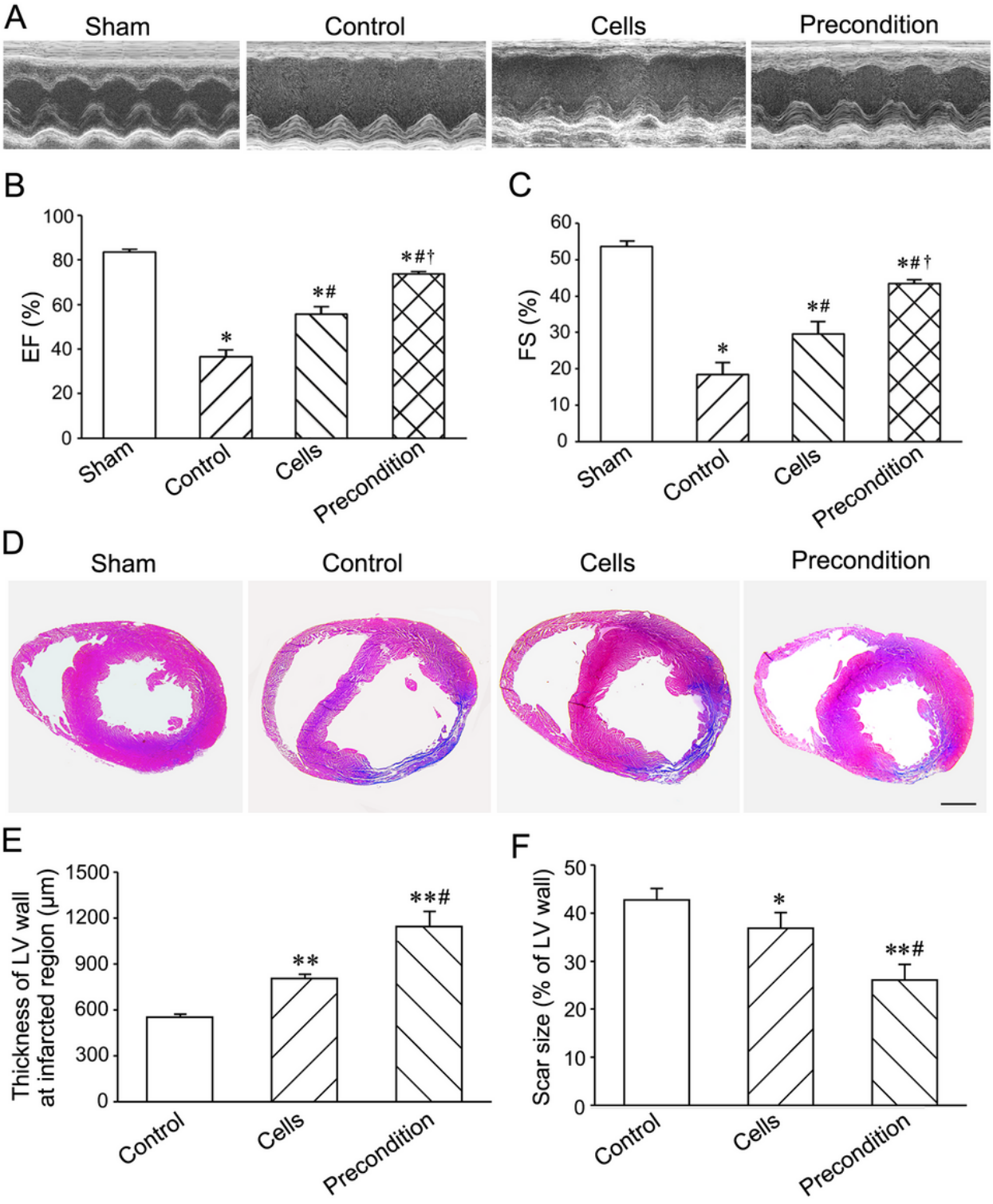

Figure 6

Changes of cardiac function and structure at 4 weeks after cell transplantation. **A** Representative echocardiograms of LV free walls. LV contraction in the precondition group is improved significantly. **B**, **C** The statistical results of EF and FS of the left ventricles. *$p < 0.05$ versus sham group, #$p < 0.05$ versus control group, †$p < 0.05$ versus cells group. **D** The transverse sections of the ventricles at the widest part of the infarct region. There is more myocardial tissue (red) and less fibrous tissue (blue) in precondition

group than cells group. Masson's trichrome staining. Scale bar=2 mm. **E**, **F** The statistical results of the thickness of LV wall at the thinnest part of the infarct region and scar size. *$p < 0.05$, **$p < 0.01$ versus control group, #$p < 0.05$ versus cells group. n=5–6.

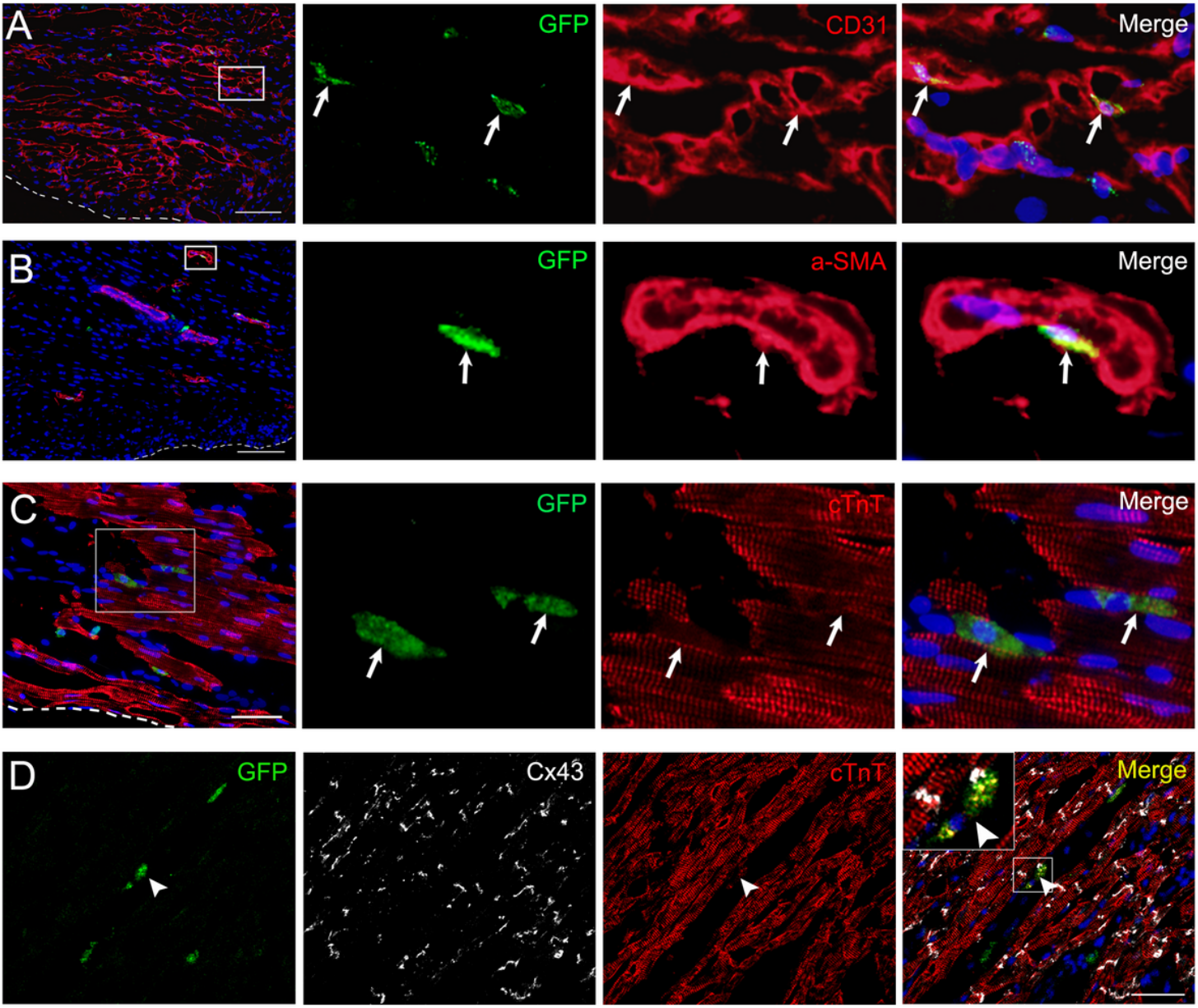

Figure 7

Differentiation of the engrafted cells at 4 weeks after transplantation. The endothelial cells (GFP^+CD31^+ cells) (**A**), smooth muscle cells ($GFP^+\alpha\text{-}SMA^+$ cells) (**B**) and cardiomyocytes (GFP^+cTnT^+ cells) (**C**) differentiated from the transplanted $c\text{-}kit^+VEGFR\text{-}2^+$ MSCs. The differentiated endothelial and smooth muscle cells are incorporated to the wall of the microvessels. In **A**, **B** and **C**, the panels from the second column to forth column are magnification of the boxes in the panels of the first column. The arrows indicate the differentiated cells. **D** Cx43 expression at the conjunction between the differentiated

cardiomyocyte and native cardiomyocyte. The large box is magnification of the small box. Scale bar=50 μm.

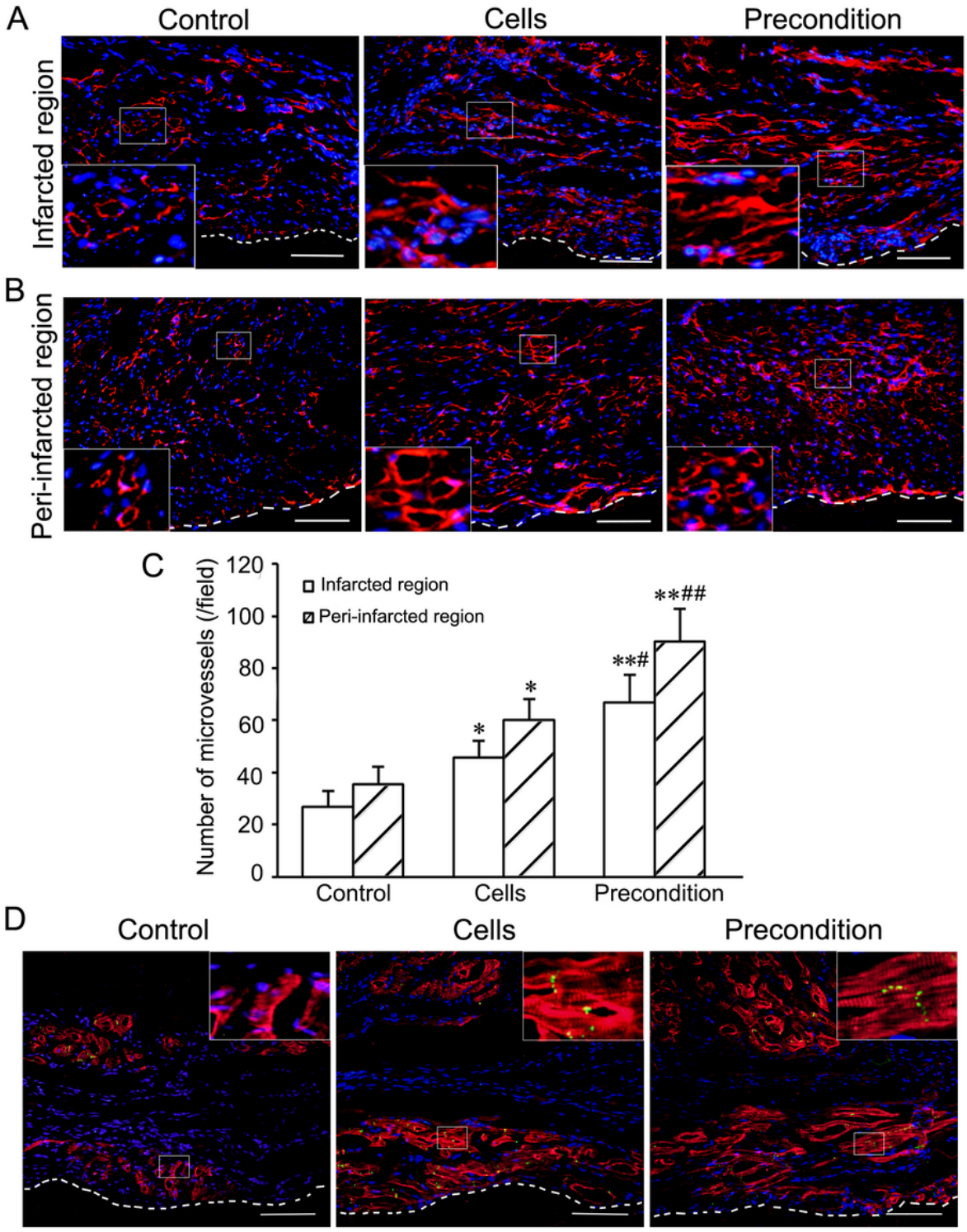

Figure 8

Angiogenesis and myocardium regeneration at 4 weeks after transplantation. **A**, **B** $CD31^+$ microvessels at the infarct and peri-infarct regions. **C** The statistical result of the numbers of the microvessels. *$p < 0.05$,

$p < 0.01$ versus control group. #$p < 0.05$ and ##$p < 0.01$ versus cells group. n=5–6. **D The myocardium and $Cx43^+$ conjunctions of cardiomyocytes at the infarcted region. In precondition group, the myocardium and $Cx43^+$ conjunctions is increased significantly. The large boxes are magnification of small boxes. Scale bar=100 μm.

Supplementary Files

This is a list of supplementary files associated with this preprint. Click to download.

- SUPPLEMENTARYMATERIALSHaijieWang.doc